THE 3D FIGURE AND SURFACE OF PALLAS FROM HST. B. E. Schmidt,[1] P. C. Thomas[2], J. M. Bauer[3], J.-Y. Li[4], S.C. Radcliffe[5], L. A. McFadden[4], M. J. Mutchler[6], J. Wm. Parker[7], A. S. Rivkin[8], C. T. Russell[1], and, S. A. Stern[9]. [1]UCLA-IGPP (britneys@ucla.edu), [2]Cornell University, [3]JPL, [4]University of Maryland, [5]Hydraulx, [6]STScI, [7]SWRI, [8]APL, [9]LPI.

Introduction: Spatially resolved images provide the ability to examine both the surface and the shape of planetary objects. Observing from Earth provides limited spatial or shape information for most asteroids due to their small extent. However, remote sensing has advanced by leaps and bounds our understanding of the largest asteroids [e.g. 1,2].

We observed 2 Pallas with Hubble Space Telescope's (HST) WFPC2 camera in September of 2007, obtaining 45 spatially resolved photometric images in 5 filters from the NUV through the Visible. Observing from space offers the advantage of a stable thermal environment, so that our images achieve resolution near WFPC2's 0.046" per pixel, resulting in about 73 km/pixel scale in the final images. These images were then deconvolved using the Maximum Entropy Method (MEM) [3].

3D Modeling: Initially, we derive a triaxial mean shape model of 291 x 278 x 250 +/- 9 km using only the raw data [3]. This method precludes any artifacts that may be introduced by deconvolution. Using this model as a basis, we then took two approaches to constructing and validating a three dimensional model.

Comparing the deconvolved to the unprocessed images, Pallas' shape and the details of its terminator are more clear after the image processing. From the images we observe Pallas' terminator to be irregular, and its shape changes significantly through the course of its rotation. In order to visualize how the changing terminator and rotation affect the appearance of Pallas at this epoch and to interpolate between frames, we utilize the Maya digital modeling software. We began with a digital triaxial ellipsoid of the dimensions given above and our pole solution, RA 42 DEC -12 [4]. We then overlay the processed image with the digital figure and fit the edge of the model to Pallas' limb by hand. We then rotate the model to the next sub-earth longitude and fit the model to the next image, repeating for each of the images and creating a full 3D asteroid from our data. In Figure 1 we show sample views of the processed images along with the digital model.

We also extracted contours from both the raw and processed images to compare and refine the model. A similar technique was used to build a digital topography model for Vesta [1]. We utilize the mean shape and contours as a comparison for the digital model. However, our image resolution is less than that of [1] since Pallas is further from the Earth than Vesta. But these two techniques are complementary and yield a model that fits our data well.

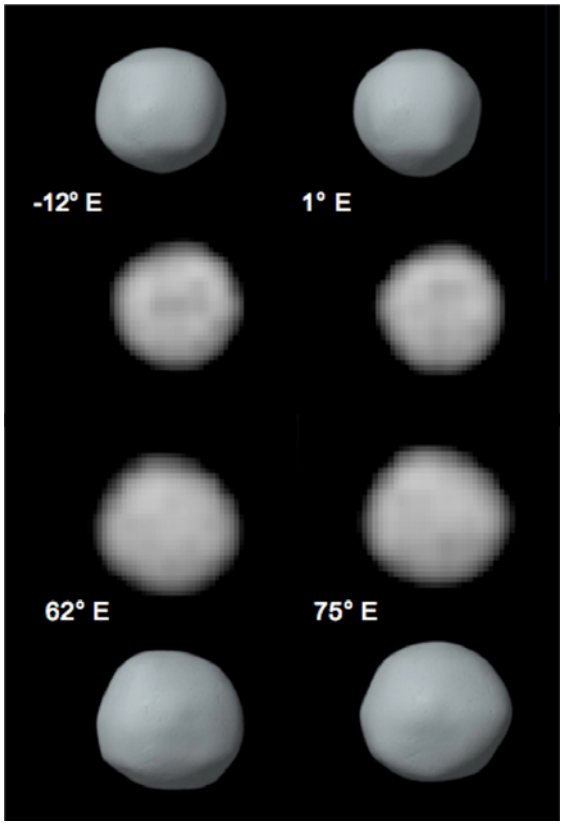

Figure 1: Comparison of 3D model to processed images. The figures are shown with north pole up with sub-Earth point near -29°.

Surface Variation and Maps: Because our images are also of good photometric quality, we obtain Pallas' average albedo and colors from whole-disk photometry and then use our processed images to construct surface maps. These maps are constructed in the NUV at 336nm and B at 435 nm. These are the first NUV and Visible surface maps of Pallas, and follow the approach used for HST mapping of Ceres [2].

Signals from disk-integrated photometry. The maximum light curve amplitude in U is 0.113 +/- 0.002 magnitudes, while it is 0.091, 0.090, and 0.088 +/- 0.002 magnitudes in B, V and I respectively. The amplitude in R is slightly lower at 0.081 +/- 0.002. With its b/a axis ratio of 0.96, this is roughly consistent with the amplitude of the B,V,R, and I light curves deriving mainly from Pallas' shape with a small com-

ponent due to spatial variation. However, the amplitude in the UV light curve is over twice that expected, suggesting a bright region near -80°, and it shape suggests a dark "spot" at 70°. We use the photometry for "ground truth" and compare this result to the surface maps.

Surface Maps. We produced maps of Pallas' surface using the center-most pixels from each of our deconvolved images to avoid geometric effects close to the limb. Because our images overlap with one another and cover nearly a full rotation of the body, we can calibrate the map using both the light curve and color data and the change in position of features as Pallas rotates. Those features that are 1) larger than a WFPC2 pixel and 2) are repeated in subsequent images are assumed to be "real." Other features, while possibly real, cannot be reliably distinguished from this data. In Figure 2 we show the NUV map of Pallas along with its regionally averaged U-V colors as a guide to determining which regions are NUV albedo features. The color plot is helpful because it compares the brightness of the surface at two wavelength while minimizing the contribution of Pallas' triaxial shape.

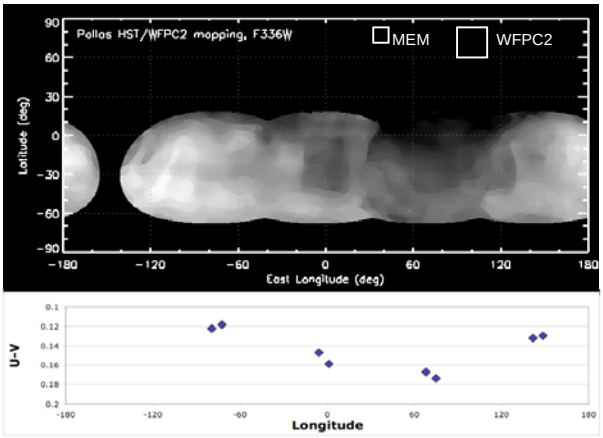

Figure 2: Surface Map of Pallas in NUV. This map has been stretched to +/- 20% contrast. The actual albedo variations are ~ +/- 10% with respect to the disk-average. The relative pixel scales of the raw WFPC2 data (73 km/pixel) and the deconvolved MEM images are shown at the top. "Real" features are those that are larger than a WFPC2 pixel, and hemispheric trends agree with the disk-averaged photometry.

The actual brightness variations across the surface are of order +/- 10%, but the map has been stretched to enhance the contrast. The region of Pallas centered near longitude 70° is dark, and the region about -90° is comparatively bright as is predicted by the light curve and colors. Bright spots near lat/lons -15°,-170° and -45°, -110° and a dark spot at -30°, 0° are visible in the map that are comparable in size to a WFPC2 pixel, and are thus possibly real.

Conclusions: Using spatially resolved images from HST, we are able to construct a three dimensional model and surface maps for Pallas. The 3D model suggests, using just Pallas' limbs, the possible existence of several topographic features, including 2 candidate "basins." The most probable "basin" appears along the limb of the image at -82° E, and is reproduced in subsequent images. This feature has an approximate scale of 200 km and is seen in the figure above as the depression in the body center of the model at 75° E. Additionally, this feature may correspond with the photometrically dark hemisphere in the surface map in Figure 2. Overall, we are gaining a better picture of the current state and history of Pallas using the unique capabilities of HST.

References:

[1] Thomas, P.C. et al. (1997) *Science 277*, 1492–1495. [2] Li J.-Y. et al. (2005) *Icarus 183*, 143-160. [3] Wu, N. (1993) *ADASS II 52*, p. 520. [4] Schmidt B. E. (2008) *LPS XXXIX* #1391, p.2502.

Additional Information: Thank you to STSCI and the Dawn mission for supporting this work.